Manufacturing and Mechanical Behavior of Hybrid Building Materials

G. C. Papanicolaou, G. Lagas, K. Papadimitropoulos, A. Ioannou

Composite Materials Group, Department of Mechanical and Aeronautics Engineering, University of Patras, GR-26500, Patras, Greece

Received 28 December 2010; accepted 6 February 2011
DOI 10.1002/app.35093
Published online 12 October 2011 in Wiley Online Library (wileyonlinelibrary.com).

ABSTRACT: This work is an experimental investigation of the flexural properties of hybrid matrix composites reinforced with different types of reinforcement, namely short glass fibers, glass beads, and short steel fibers. The aim of this investigation is to determine the mechanical behavior and properties of the composites that were manufactured, as well as to define an optimum composition of the materials used that will result in a composite with enhanced mechanical performance for building applications. © 2011 Wiley Periodicals, Inc. J Appl Polym Sci 124: 1081–1095, 2012

Key words: composite; matrix; fibers; reinforcement; electron microscopy

INTRODUCTION

The use of polymer matrix composite building materials in the field of construction has been rapidly increased in the last decade. The main reason for this turn to composite materials, apart from the desirable mechanical properties that they exhibit, is their excellent corrosion durability,[1] as well as the fact that they are easily applicable especially on strengthening and repair applications. On the contrary, conventional cement-based building materials do not exhibit such behavior mainly because of their high porosity, which allows corrosion procedures, such as carbonation, to occur.[2] Additionally, and as a result of its high specific weight, use of conventional concrete leads to high dead loads added to the structure. In recent years, a common practice is polymer matrix composites to be used for a variety of strengthening and repair applications, such as steel rebars anchoring on existing concrete members, where a mixture of epoxy resin and quartz aggregates is used, and crack filling on concrete members where low viscosity resin is injected in the crack.[3]

Moreover, the use of fiber reinforced polymers (FRPs) is quite extended in the field of strengthening of existing structures, since they can be utilized in cost and time effective methods of application. Taking into account parameters such as the loads that must be delivered, the type of material that structure members are consisting of (concrete,[4] wood,[5] steel,[6] masonry walls[7]) and the environmental conditions that they will be subjected to,[8] different fiber materials and forms of FRPs are used. A variety of fabrics with unidirectional or bidirectional orientation of carbon or glass fibers are available,[9] applied by the use of epoxy resin as bonding material. Also, carbon fiber reinforced polymers (CFRPs) can be found in the form of straight[10] or L-shaped prefabricated plates[11] that are bonded on the existing structure members by the use of epoxy resin as well, while much research work has been made in the field of use of CFRP rods[12] as reinforcement in concrete structural members.

It is obvious from all the above that is of particular interest the investigation of the behavior of polymer-matrix composite materials reinforced with various types of reinforcement. The purpose of this investigation should be the development of new building materials with enhanced mechanical properties.

In this experimental investigation, epoxy resin and fine marble sand are mixed in different by weight ratios formulating different hybrid matrices. These hybrid matrices are tested mechanically by means of three-point bending test. Their mechanical (flexural) properties and behavior are studied before and after the addition of different types of reinforcement (glass beads, short glass fibers, and short steel fibers) at different by weight ratios. Furthermore, the specimens manufactured were optically observed by means of images obtained by SEM (Scanning Electron Microscopy) and the correspondence of the optical findings with the mechanical behavior is discussed.

Correspondence to: G. C. Papanicolaou (gpapan@mech.upatras.gr).

MATERIALS AND EXPERIMENTAL

The materials used for the manufacturing of the hybrid matrix were epoxy resin and fine marble sand mixed in three different compositions. Hybrid matrices were reinforced with three types of reinforcement namely short glass fibers ($l = 3$ mm, $r_f = 14$ μm), glass beads ($d = 75$–150 μm) and short steel fibers ($l = 6$ mm, $r_f = 180$ μm). The following Table I gives a complete overview of the compositions that were manufactured and tested. All percentage content of the materials is by weight.

A standard manufacturing procedure was held for all compositions. The first step was the removal of humidity from marble sand. This was necessary since commercial, plain marble sand was used, which is stored in piles outdoors and may have large water content. For this purpose marble sand was put in an oven for 24 h at a temperature of 50°C. Through this treatment, all the excessive humidity was expelled from the marble sand, resulting to improved adhesion between epoxy resin and marble sand particles.

Mixing procedure was initiated by the homogenization of the solid ingredients (marble sand, fibers or beads) and then the liquid part (resin) along with the proper amount of amine added. The overall mixing time was kept constant and equal to 5 min. Then, the mixture was set in a vacuum chamber for a period of 5 min in order that the air resulted from the mechanical mixing to be removed out of the mass of the composite. Finally, the mixture was casted in open molds and the curing process of the specimens consisted of 24 h heating in an oven at a constant temperature of 50°C. The nominal dimensions of the molds were 100.00 mm in length, 12.90 mm in width, and 3.00 mm in thickness.

After curing process was completed, specimens dimensions were measured again in order the exact "as manufactured" dimensions to be available for stress and strain calculation.

Next, three-point bending tests were executed according to ASTM D790-99. A data acquisition system was used to monitor data and transform force-displacement curves, onto stress–strain curves from which both flexural modulus and strength values were accurately determined. For each composition a total number of six specimens were manufactured, and a mean value of each of the aforementioned mechanical properties was derived as the average value of all specimens tested.

RESULTS AND DISCUSSION

Mechanical properties and behavior

Unreinforced matrices

The following Figure 1 shows three typical experimental stress–strain curves, one for each hybrid matrix composition that was manufactured and tested before any reinforcement was added.

A strong relationship between resin content and flexural strength is obvious. As the resin content increases, an increase in flexural strength is evident. This is due to the fact that as more resin is added in

TABLE 1
Overview of Compositions Manufactured and Tested (V: tested x: not tested)

Hybrid matrix	Resin (% w_f)	Marble Sand (% w_f)	Reinforcement (% w_f)	Glass fibers	Glass beads	Steel fibers
60% Marble Sand 40% Epoxy resin	40.00	60.00	0.00	√	√	√
	38.00	57.00	5.00	√	√	√
	36.00	54.00	10.00	√	√	√
	34.00	51.00	15.00	√	√	√
	32.00	48.00	20.00	×	×	√
	30.00	45.00	25.00	×	×	√
	28.00	42.00	30.00	√	√	√
70% Marble sand 30% Epoxy resin	30.00	70.00	0.00	√	√	√
	28.50	66.50	5.00	√	√	√
	27.00	63.00	10.00	√	√	√
	25.50	59.50	15.00	√	√	√
	24.00	56.00	20.00	×	×	√
	22.50	52.50	25.00	×	×	√
	21.00	49.00	30.00	√	√	√
80% Marble sand 20% Epoxy resin	20.00	80.00	0.00	√	√	×
	19.00	76.00	5.00	√	√	×
	18.00	72.00	10.00	√	√	×
	17.00	68.00	15.00	√	√	×
	16.00	64.00	20.00	×	×	×
	15.00	60.00	25.00	×	×	×
	14.00	56.00	30.00	√	√	×

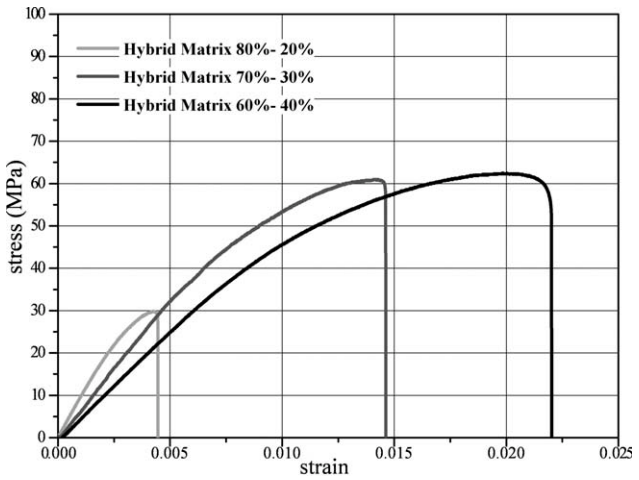

Figure 1 Typical stress–strain curves for unreinforced hybrid matrices (polymer and marble sand) manufactured and tested.

the composite a better impregnation of marble sand is achieved, fewer voids are generated; and therefore, a more effective load transfer regime is established between sand particles and resin. On the other hand, increased resin content leads to a proportional increase in the average distance between marble sand particles. As interparticle distance increases more resin, which is characterized by low stiffness, is positioned in the space between marble sand particles formatting a longer, and therefore a less stiff connection between them. As a result, a decrease in modulus of elasticity and an increase in the failure strain were observed as increase in resin content leads to a less brittle material with more ductile behavior. The validity of the aforementioned suggestion on the effect of resin content on the mechanical properties of the manufactured materials relies on the assumption that the resulting composite material is homogenous, i.e., resin and marble sand are equally distributed in the mass of the composite. Later in this work it will be proved that the resulting materials are not homogenous for all marble sand to resin, by weight, content ratios. Nevertheless, as it will be seen in following paragraphs, mechanical properties of the hybrid matrices can be predicted, with no remarkable errors, under the hypothesis of homogeneity.

Glass fibers reinforcement

Glass fibers reinforcement does not seem to have any enhancement effect in stiffness values that were found [Fig. 2(a,b)]. For the 80–20% matrix, addition of reinforcement more than 10% led to a degradation of the modulus of elasticity. This behavior can be justified by the lack of adequate quantity of resin enough to impregnate the solid parts of the composite (sand particles and glass fibers). Moreover, it seems that glass fibers of that kind and with this method of mixing cannot be fully homogenized in the composite and many areas of voids and discontinuities are created, resulting to flexural strength degradation as Figure 3(a,b) shows.

Glass beads reinforcement

Glass beads addition has an enhancement effect on modulus of elasticity, which manifests after a minimum reinforcement loading is added [Fig. 4(a,b)]. This minimum reinforcement load is different for each hybrid matrix composition. For hybrid matrix consisting of 80 wt % marble sand–20 wt % resin enhancement effect becomes evident after 2.50% per weight reinforcement is added and for the 70–30% and 60–40% hybrid matrices this minimum reinforcement loading is 5.00 and 10%, respectively. For the 80–20% hybrid matrix, maximum enhancement

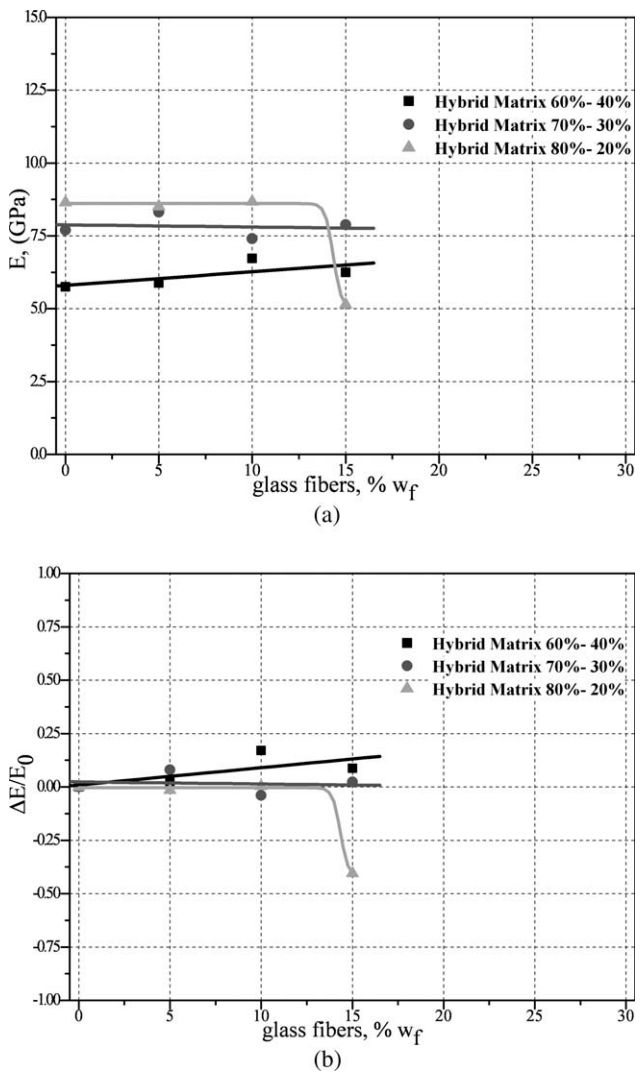

Figure 2 (a) Variation in stiffness with glass fibers reinforcement loading. (b) Relative variation in stiffness with glass fibers reinforcement loading.

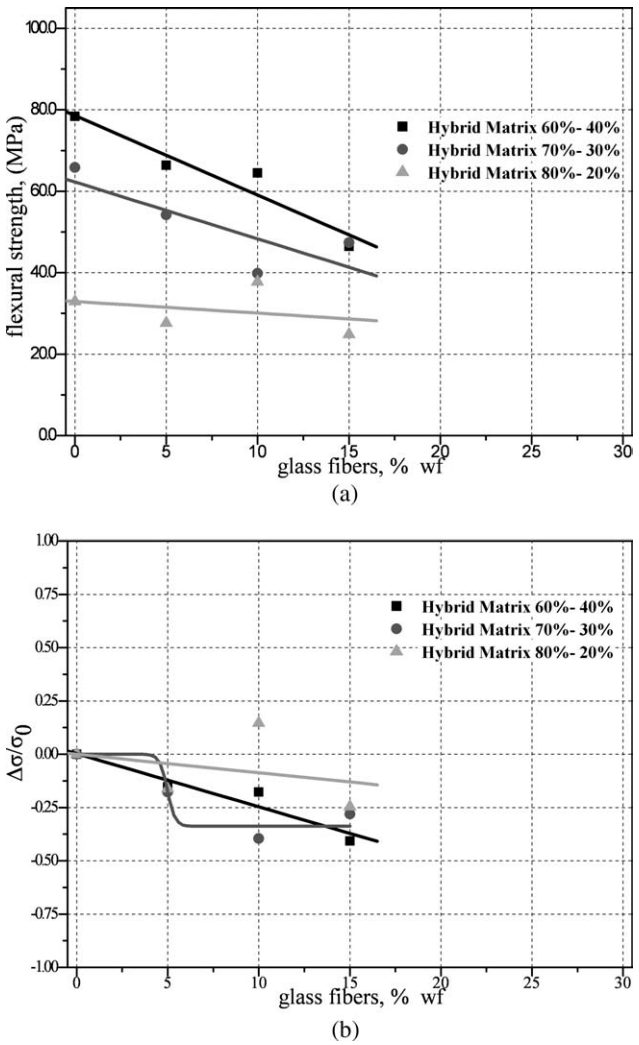

Figure 3 (a) Variation in flexural strength with glass fibers reinforcement loading. (b) Relative variation in flexural strength with glass fibers reinforcement loading.

occurred when 7.50% by weight reinforcement was added. In that case, stiffness was found to be more than 25% higher than the one that was experimentally found by testing the unreinforced hybrid matrix.

Optimal enhancement of stiffness of the 70–30% and 60–40% hybrid matrices was achieved by adding 20 and 30% by weight glass beads reinforcement, respectively. The 70–30% matrix found to have stiffness increased by 21% in that case, whereas the stiffness of the 60–40% hybrid matrix reached an increase equal to 33% comparing to the values found after testing the unreinforced hybrid matrices.

Addition of glass beads does not seem to have any reinforcement effect on flexural strength in all cases [Fig. 5(a,b)]. Moreover, when by weight reinforcement content exceeded 15%, flexural strength showed an abrupt degradation, possibly due to the presence of voids and agglomerations caused by the fact that resin quantity was insufficient to impregnate the inclusions properly. Therefore, stress concentration areas were created around these anomalies and failure occurred at lower load levels.

Steel fibers reinforcement

Figures 6(a,b) show the stiffness variation of 60–40% and 70–30% marble sand/epoxy resin hybrid matrices reinforced with various by weight content of steel fibers reinforcement. The evident reinforcing effect is triggered after a minimum reinforcement content, which is different for every hybrid matrix, is added in the composite. This minimum value is 5 and 10% for the 60–40% and 70–30% hybrid matrix, respectively. The optimum reinforcing effect is taking place when 20% by weight reinforcement is added for both hybrid matrices. Stiffness of both reinforced hybrid matrices in that case is increased almost by 68%, comparing to the unreinforced ones.

An enhancement effect of steel fibers reinforcement is obvious on the flexural strength of the specimens that

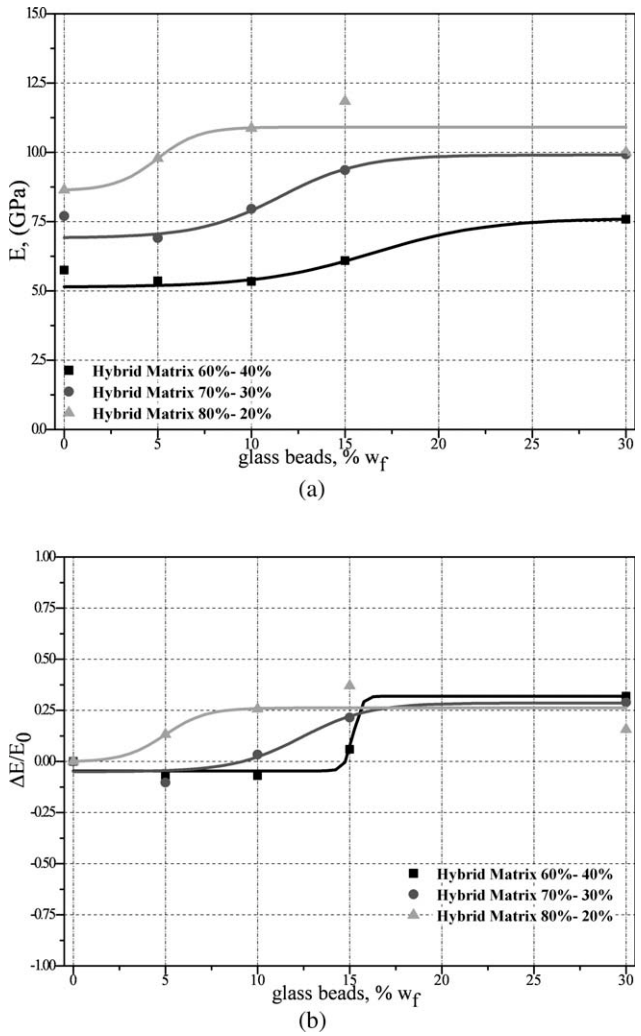

Figure 4 (a) Variation in stiffness with glass beads reinforcement loading. (b) Relative variation in stiffness with glass beads reinforcement loading.

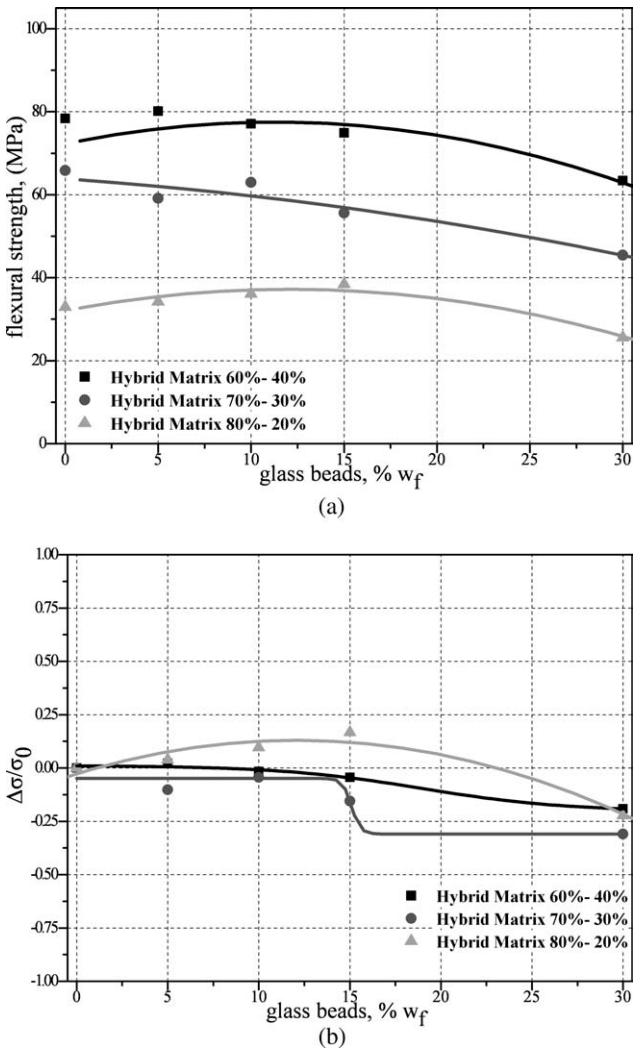

Figure 5 (a) Variation in flexural strength with glass beads reinforcement loading. (b) Relative variation in flexural strength with glass beads reinforcement loading.

were tested as Figure 7 shows. Reinforcement effect becomes obvious on both hybrid matrices after 10% by weight steel fibers were added. A peak is reached when $\sim$ 20% by weight steel fibers are added in both cases. The value of the flexural strength at the peak are, for the 60–40% case, 28% higher than the one found on the unreinforced matrix, whereas for the 70–30% hybrid matrix the value of stiffness increase was found to be approximately equal to 15%.

For reinforcement content higher than 20%, and for reasons already stated, both stiffness and flexural strength degrade rapidly and reach the values of the unreinforced hybrid matrices when 30% by weight steel fibers are added in the composite.

From the above short summary of the experimental results, it is obvious that 20% by weight steel fibers reinforcement added to the hybrid matrices considered has a remarkable enhancement effect on the mechanical properties tested in this work. Following Figures 8 and 9 show typical, experimental stress–strain curves, one for the 60–40% hybrid matrix reinforced with 20% by weight steel fibers and one for the 70–30% hybrid matrix containing the same reinforcement loading.

These figures depict the enhancement effect for both stiffness and flexural strength of 20% by weight steel fibers addition in the composite. Comparing the two figures we can conclude that the relationship between resin content and flexural strength/stiffness, which was discussed earlier for the unreinforced hybrid matrices, is also valid for the reinforced hybrid matrices: As resin content increases flexural strength increases as well, while stiffness degrades. In addition, an observation of the figures leads to the conclusion that reinforced hybrid matrices have lower failure strain than the corresponding unreinforced. The reason for this behavior might be the fact that when strain reaches a certain value, fibers are debonding and losing contact from hybrid

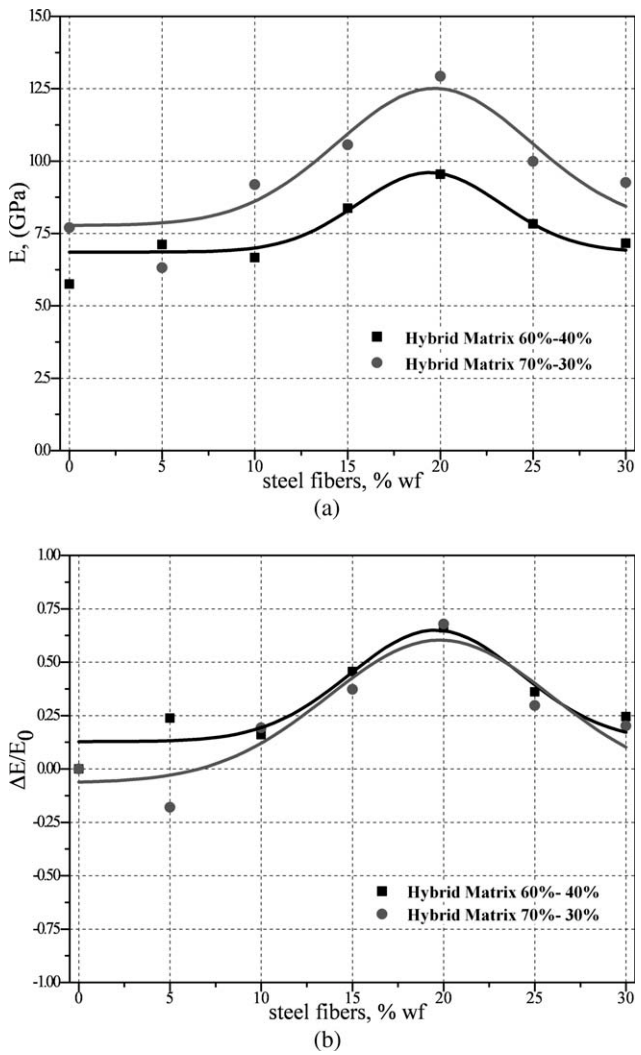

Figure 6 (a) Variation in stiffness with steel fibers reinforcement loading. (b) Relative variation in stiffness with steel fibers reinforcement loading.

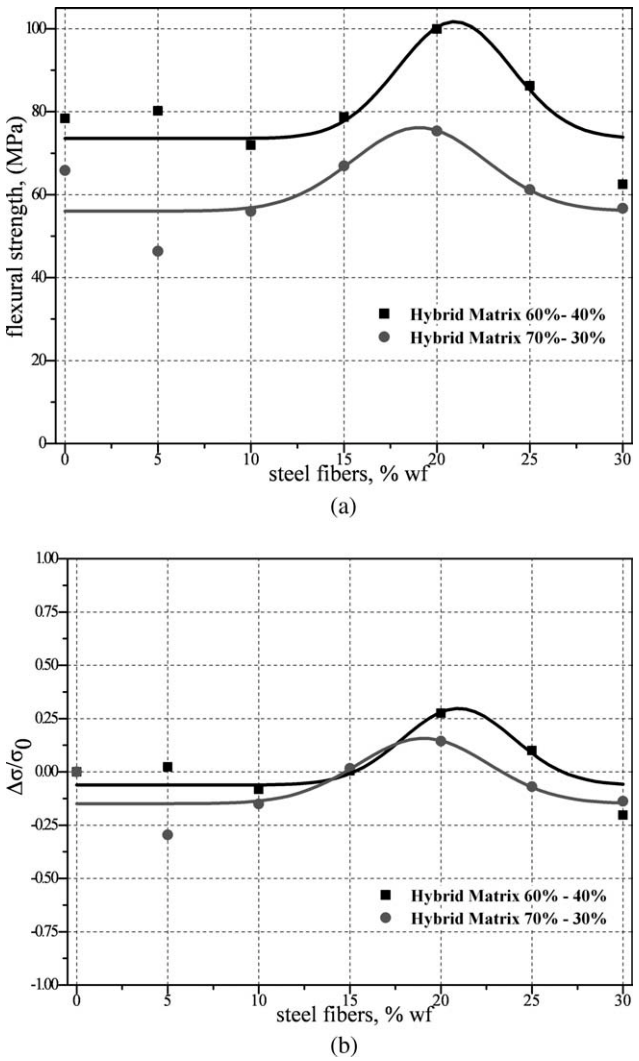

Figure 7 (a) Variation in flexural strength with steel fibers reinforcement loading. (b) Relative variation in flexural strength with steel fibers reinforcement loading.

matrix and, therefore, their load-bearing capacity is degrading. Subsequently, load higher than its capacity is transferred through the hybrid matrix leading the specimen to failure.

Modeling of stiffness

A number of analytical models were used to reproduce the stiffness values of the materials that were tested. Considering the assumption that all matrices and inclusions involved exhibit linear elastic behavior, rule of mixtures [Eq. (1)][13] was used for predicting modulus when loading is parallel to the fibers (E_1) and Eq. (2) for predicting transverse modulus (E_2).[13]

$$E_1 = E_{||} = E_f V_f + E_m(1 - V_f) \tag{1}$$

$$E_2 = E_{\perp} = \frac{E_f E_m}{E_f(1 - V_f) + E_m V_f} \tag{2}$$

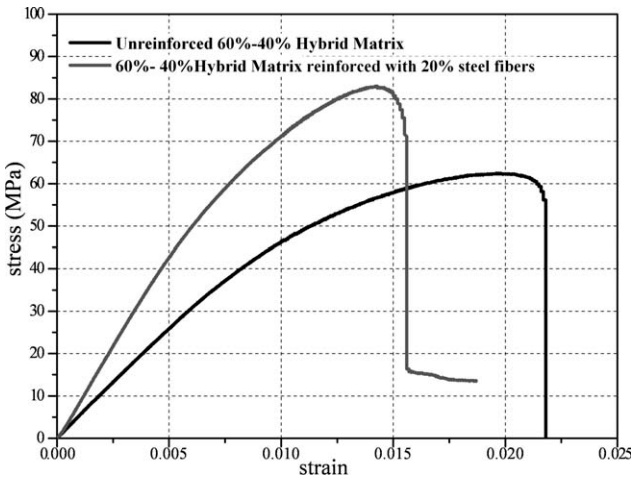

Figure 8 Typical, experimental stress–strain curves for 60–40% hybrid matrix reinforced with 20% by weight steel fibers.

where: E_f,V_f: Stiffness and by volume content, respectively, of inclusion, E_m: Stiffness of matrix.

Furthermore, Halpin–Tsai equations[13] were used as given below:

$$\frac{E_c}{E_m} = \frac{1 + \xi\eta V_f}{1 - \eta V_f} \tag{3}$$

With

$$\eta = \frac{\frac{E_f}{E_m} - 1}{\frac{E_f}{E_m} + 1} \tag{4}$$

where: E_f,V_f: Stiffness and by volume content of inclusion, E_m, E_c: Stiffness of the matrix and the composite, respectively.

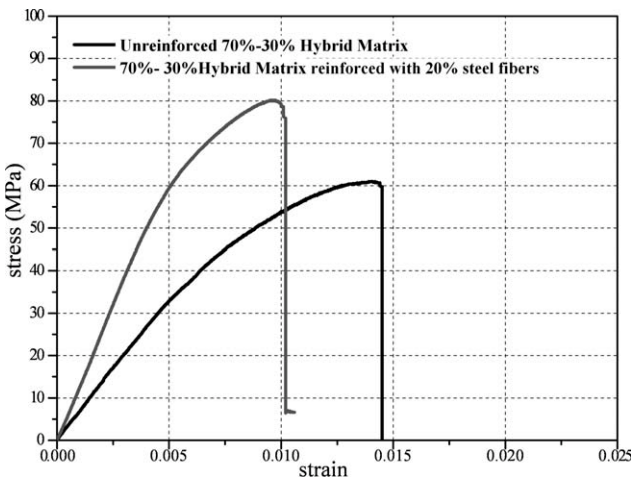

Figure 9 Typical, experimental stress–strain curves for 70–30% hybrid matrix reinforced with 20% by weight steel fibers.

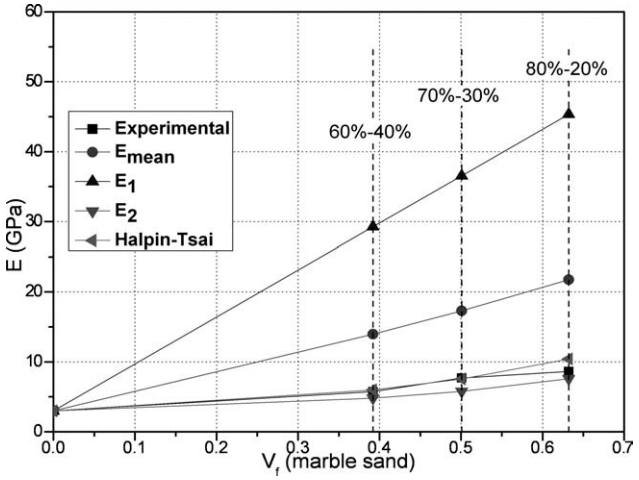

Figure 10 Modeling the stiffness of unreinforced hybrid matrices.

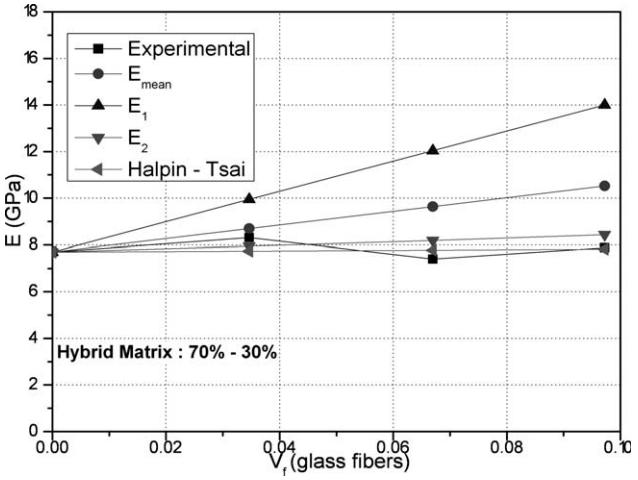

Figure 12 Modeling the stiffness of 70–30% hybrid matrix reinforced with glass fibers.

Finally, a simplified expression used for modeling the value of modulus of composites consisting of impregnated resin into a long fiber chopped-strand mat[13] under the assumption uniform probability distribution of fibers over the entire range of angles from -90° to $+90^\circ$ was utilized to predict the values of modulus for different by volume contents of the composites that were investigated.

$$E_{mean} = \frac{3}{8}E_1 + \frac{5}{8}E_2 \tag{5}$$

where: E_1, E_2 derived from expressions (1) and (2), respectively.

Modeling the stiffness of the unreinforced hybrid matrices

The stiffnesses of the hybrid matrices that were manufactured and tested were modeled by means of the above equations. By weight contents were converted to volume fractions, considering densities of marble and resin to be $\rho_{resig} = 1.10$ g/cm^3 and $\rho_{marble} = 2.56$ g/cm^3, respectively. The value of the modulus of pure resin was determined experimentally and was found to be $E_{resin} = 3.00$ GPa while the modulus of marble (E_{marble}) was considered to be equal to 70.00 GPa. Setting V_f equal to the volume fraction of marble sand and considering $E_f = E_{marble}$ and $E_m = E_{resin}$, the values of the expressions (1), (2), and (5) are calculated.

For the application of the Halpin–Tsai equation, fitting over the experimental data points was conducted ξ to determine the parameter. Then, the value of the ξ parameter determined was set in Eq. (3) and the model values for modulus were calculated.

Following Figure 10 shows the results of the calculations described above along with the experimental

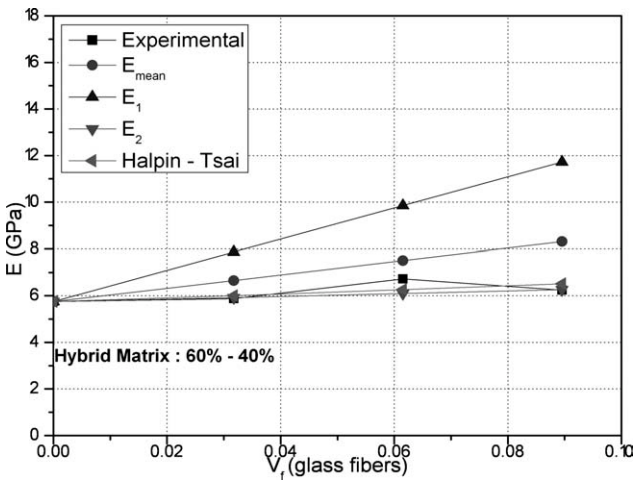

Figure 11 Modeling the stiffness of 60–40% hybrid matrix reinforced with glass fibers.

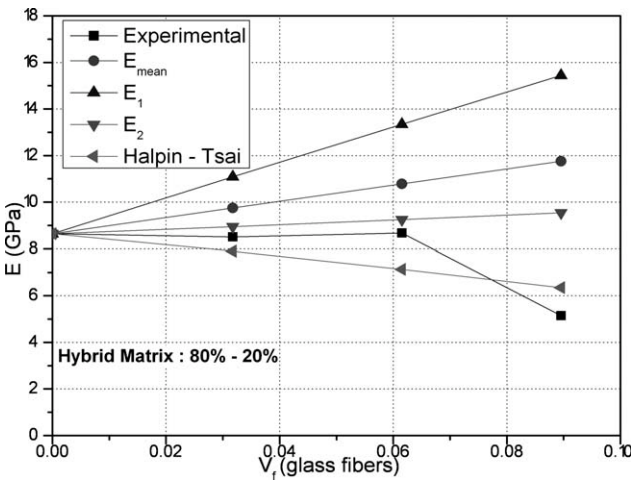

Figure 13 Modeling the stiffness of 80–20% hybrid matrix reinforced with glass fibers.

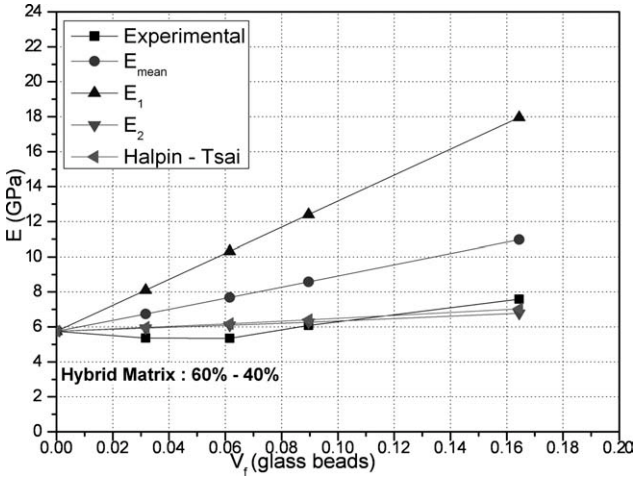

Figure 14 Modeling the stiffness of 60–40% hybrid matrix reinforced with glass beads.

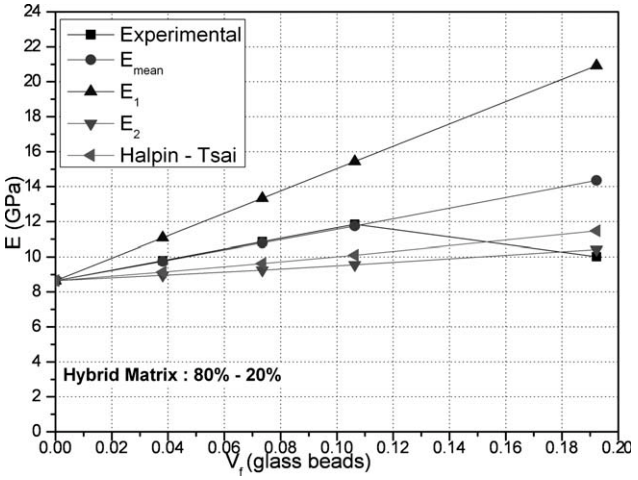

Figure 16 Modeling the stiffness of 80–20% hybrid matrix reinforced with glass beads.

values of the stiffness of the hybrid matrices that were manufactured and tested. As it can be obtained from the figure, Halpin–Tsai equation gives a very good approximation of the values of the modulus that were experimentally determined, while lower bound (E_2) line was found to be also quite close to them. On the contrary, values that were calculated by using rule of mixtures and by the expression (5) (E_{mean}) present a significant deviation from the measured valued.

Modeling the stiffness of the reinforced hybrid matrices

The modeling procedure that was described above was also applied to the composites that were manufactured by reinforcing the three types of hybrid matrices (60–40%, 70–30%, 80–20% by weight) with various types of reinforcement, namely short glass fibers, short steel fibers and glass beads. By weight ratios were transformed to volume fractions using density values equal to 2.55 g/cm^3 and 7.80 g/cm^3 for the densities of E-glass and steel, respectively. The modulus value used for glass was $E_{\text{glass}} = 72.50$ GPa, whereas for steel the corresponding value was $E_{\text{steel}} = 200.00$ GPa. Modulus of the matrix was the modulus of each hybrid matrix that was each time considered ($E_{60-40\%} = 5.75$ GPa, $E_{70-30\%} = 7.70$ GPa, $E_{80-20\%} = 8.65$ GPa). Again, for the application of the Halpin–Tsai equation, ξ parameter was determined by fitting the available experimental data for every hybrid matrix and for every kind of reinforcement that was used.

Following Figures 11, 12, and 13 show the results of modeling for glass fibers reinforced hybrid matrices. It can clearly be seen in 60–40% and 70–30% cases that all values are close to the lower bound (E_2) and the line representing the Halpin–Tsai equation. In the case of 80–20% hybrid matrix, it is

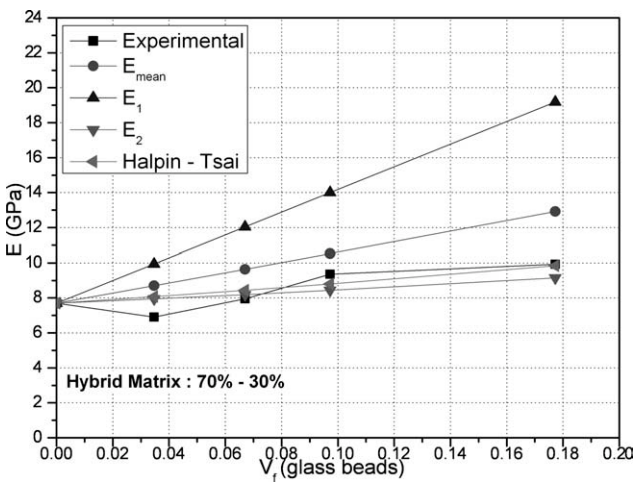

Figure 15 Modeling the stiffness of 70–30% hybrid matrix reinforced with glass beads.

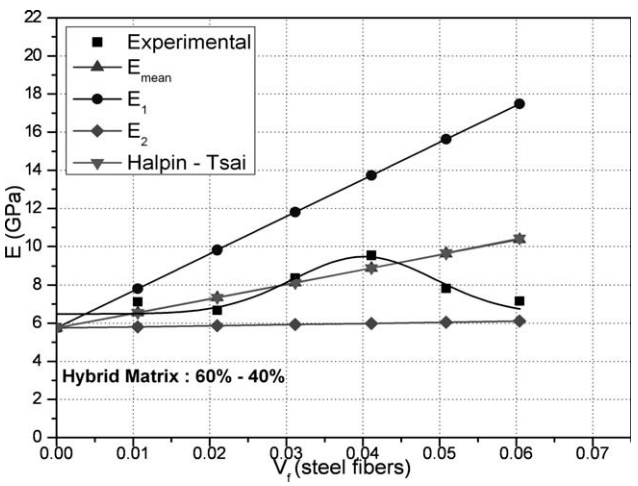

Figure 17 Modeling the stiffness of 60–40% hybrid matrix reinforced with steel fibers.

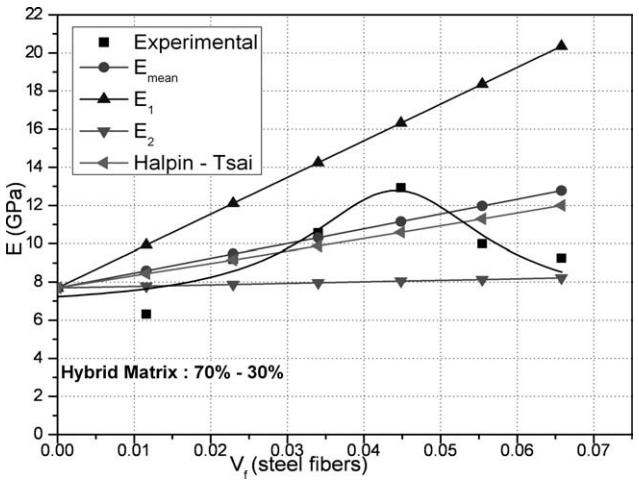

Figure 18 Modeling the stiffness of 70–30% hybrid matrix reinforced with steel fibers.

obvious that poor bonding conditions between the hybrid matrix and fibers are causing experimental values to drop significantly lower than the lower bound (E_2) line, while Halpin–Tsai equation values cannot reproduce the experimental values adequately.

Results for hybrid matrices reinforced with glass beads are shown on Figures 14, 15, and 16. For the case of 60–40% experimental values are well predicted by both the lower bound (E_2) and Halpin–Tsai equation. The same pattern of behavior can be observed for the 70–30% hybrid matrix case.

In the case of 80–20% hybrid matrix, experimental data have a very good agreement with the E_{mean} values. Last experimental point deviates from the corresponding E_{mean} value since low resin content leads to the creation of voids that caused the degradation of the composite's properties.

Finally, results for hybrid matrices reinforced with steel fibers are shown in Figures 17 and 18. Almost all data points are between the values obtained from E_1 and E_2 equations. Halpin–Tsai and E_{mean} values are quite close to the experimental values up to volume fractions that correspond to 20% by weight content for the 60–40% hybrid matrix and 15% by weight content for the 70–30% hybrid matrix. After that, for reasons stated previously, the experimental values are dropping and none of the models used is able to reproduce such behavior.

Scanning electron microscopy

For a number of characteristic compositions of those that were manufactured, additional investigations

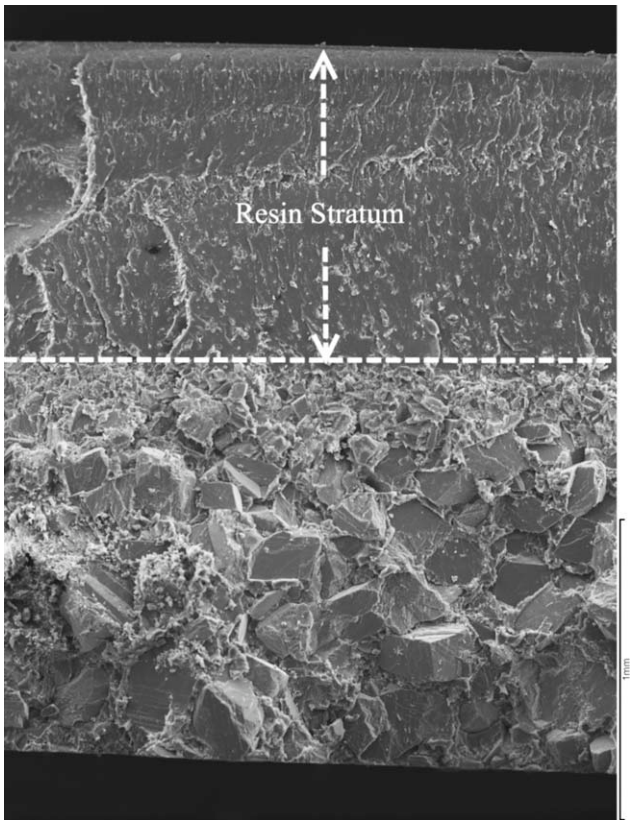

Figure 19 SEM image of cross section of the fracture surface of hybrid matrix consisting of 60% marble sand and 40% epoxy resin.

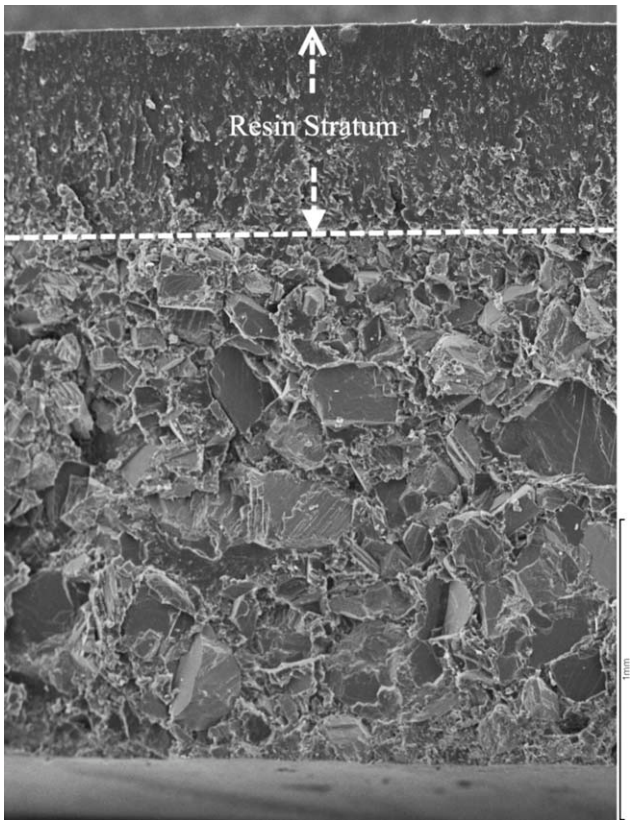

Figure 20 SEM image of cross section of the fracture surface of hybrid matrix consisting of 70% marble sand and 30% epoxy resin.

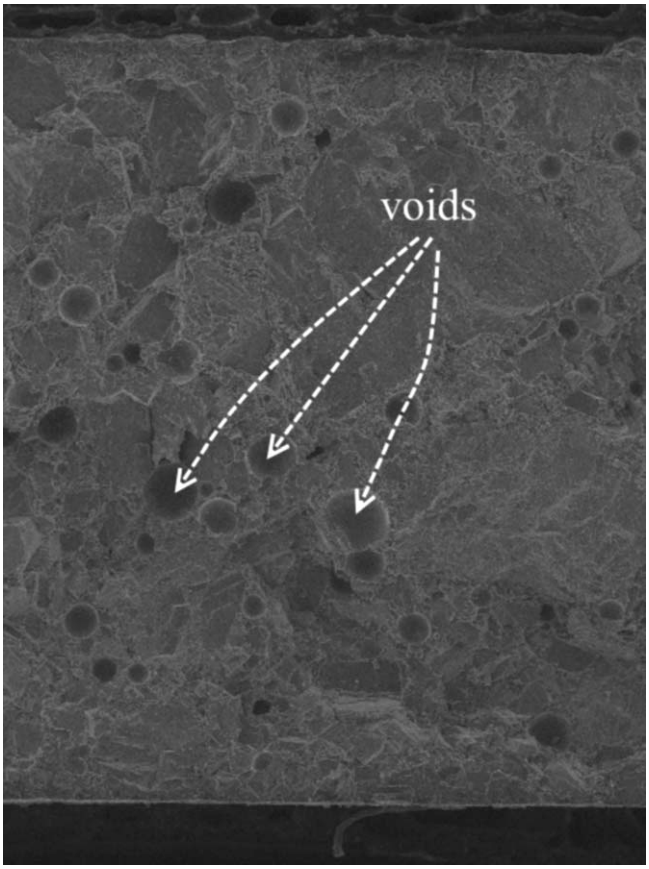

Figure 21 SEM image of cross section of the fracture surface of hybrid matrix consisting of 80% marble sand and 20% epoxy resin.

were held by means of Scanning Electron Microscope. Scanning was conducted on the fracture surface of the specimen, perpendicular to its longitudinal axis. Efficient electric conductivity was achieved by sputtering all specimens with gold before examination procedure.

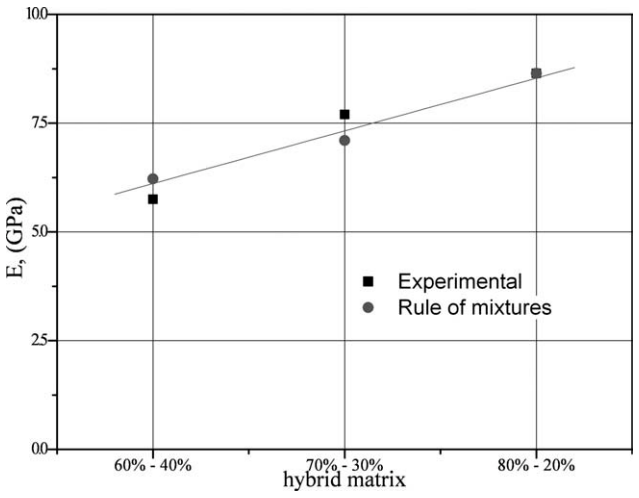

Figure 22 Rule of mixtures application results for the hybrid matrices manufactured.

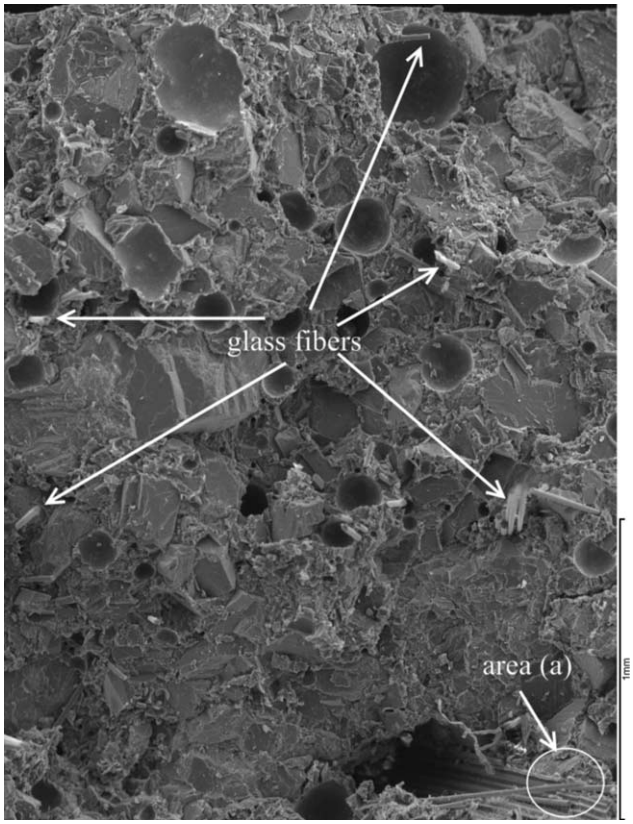

Figure 23 SEM image: Fracture surface cross section of hybrid matrix consisting of 80% marble sand and 20% epoxy resin reinforced with 5 wt % glass fibers.

Unreinforced hybrid matrices

Next, Figures 19, 20 and 21 show the structure of the hybrid matrices manufactured magnified by a magnification factor equal to 45. A strong settlement effect is obvious in the 60–40% and 70–30% hybrid matrices (Figs. 19 and 20). Solid part of the composite is settling on the bottom of the mold while a stratum of resin mixed with the finest fraction of the marble sand is positioned on the top. The thickness of the resin stratum is proportional to the by weight resin content of the hybrid matrix. On the other hand, 80–20% hybrid matrix (Fig. 21) does not show any settlement effect as solid and liquid parts of the composite are equally distributed over the mass of the composite.

Stratification, resulting from the sedimentation of marble sand after mixing with resin, shows clearly that manufacturing process does not lead to homogenous materials. Materials in the cases of 60–40% and 70–30% hybrid matrices seem to be consisting of two plies. The upper ply consists of plain resin. Lower ply consists of a mixture of resin and marble sand. In this case, voids between the marble sand particles are fully filled by the resin. This material is more or less the same with the 80–20% hybrid matrix where voids of the marble particles are filled

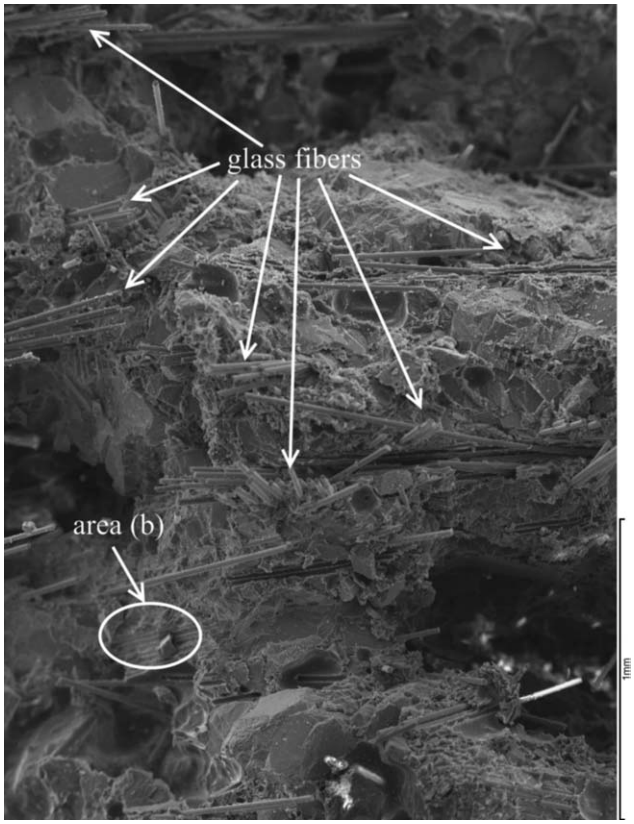

Figure 24 SEM image: Fracture surface cross section of hybrid matrix consisting of 80% marble sand and 20% epoxy resin reinforced with 15 wt % glass fibers.

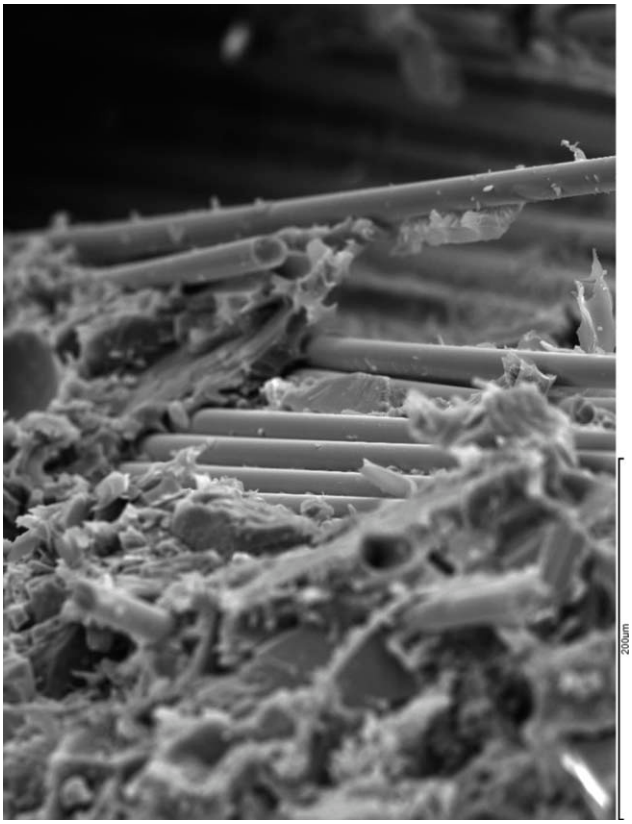

Figure 25 SEM image: Area (a)

with resin and as a result there is no resin stratum visible in the corresponding SEM image (Fig. 21). The two plies are bonded under perfect adhesion conditions. By volume content in the composite of the materials that two plies consist of, can be calculated by the ratio of the corresponding thicknesses. Taking into account that pure resin's stiffness under three-point bending tests was found equal to 3.00GPa, whereas 80–20% hybrid matrix's stiffness was found equal to 8.65 GPa rule of mixtures can be applied for 60–40% and 70–30% hybrid matrices:

$$E_{hm} = E_r V_r + E_{sat}(1 - V_r) \quad (6)$$

Where: E_r,V_r: Stiffness and by volume content, respectively, of plain resin, E_{sat}: Stiffness of mixture of resin and marble sand when voids between sand particles are fully saturated in resin (80% marble sand–20% resin by weight content hybrid matrix).

As following Figure 22 depicts, rule of mixtures results to a quite accurate approach of the stiffnesses measured during experimental procedure. Although homogeneity is a requirement for the application of rule of mixtures, we can conclude that they behave as if they were homogenous even if SEM images

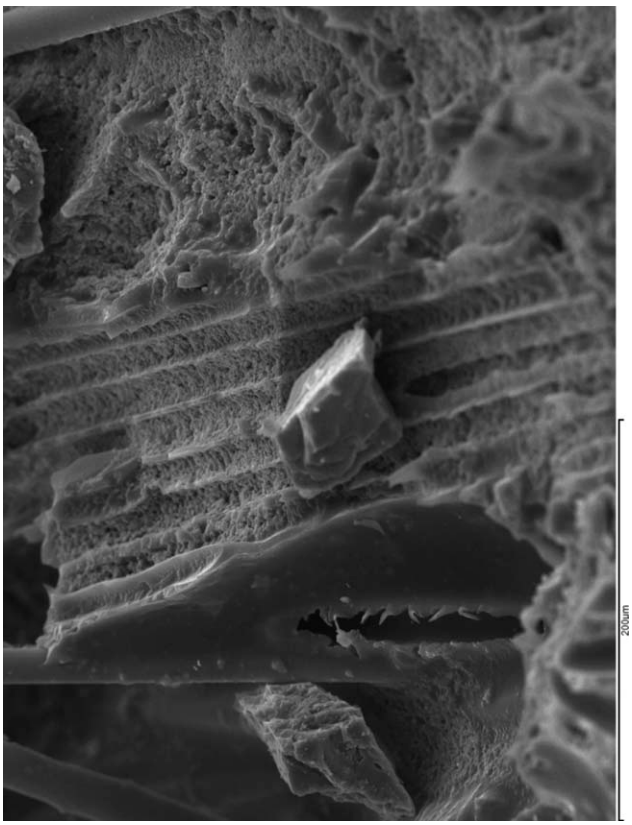

Figure 26 SEM image: Area (b)

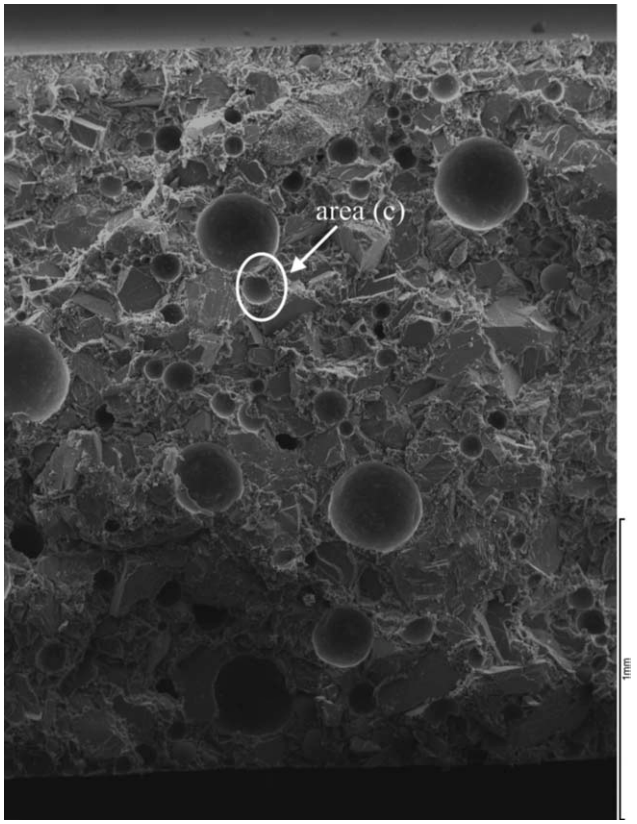

Figure 27 SEM image: Fracture surface cross section of hybrid matrix consisting of 80% marble sand and 20% epoxy resin reinforced with 5 wt % glass beads.

show a structure, which is far from being characterized as homogenous.

In all cases, good mixing conditions are evident. With an exception of the 80% marble sand–20% epoxy resin hybrid matrix in which a number of voids are visible, no voids or sand particles agglomerations are visible and therefore we can assume that resin content is adequate to fully impregnate the sand particles. The presence of voids in the 80% marble sand–20% epoxy resin hybrid matrix explains its low flexural strength that was experimentally found comparing to the flexural strength found for the other two hybrid matrices.

Hybrid matrices with glass fibers reinforcement

The experimental results derived from the glass fiber reinforced hybrid matrices can be justified by the following Figures 23 and 24. It seems that by the way of mixing used, glass fibers cannot be homogeneously distributed in the mass of the composite as they cannot be separated from the bundles that they form. Furthermore, they cannot be properly impregnated by resin and, subsequently, they are not strongly bonded to the hybrid matrix. This is obvious locally even for low (5% by weight) fiber content (Fig. 23) but in higher reinforcement loadings the effect is more dramatically manifested (Fig. 24).

Figure 25 shows the area designated on Figure 23 as area (a) magnified by a factor of 270. Voids and poor bonding conditions can be clearly seen. Around the area of the fibers, sand particles seem to form aggregates, due to the fact that a part of the resin content is locally consumed in an effort to impregnate the fibers.

The situation in the case of area (b) designated in Figure 24 is not much different. Magnifying area (b) by a factor of 300 a number of parallel paths consisting of resin and fine sand particles can be seen (Figure 26). Those paths were created after glass fibers were debonded and the trace of them was left on the hybrid matrix. It is clearly seen that the contact area between glass fibers and hybrid matrix is full of voids, as its porous look denotes, something which converges with our assumption for poor bonding conditions.

Hybrid matrices with glass beads reinforcement

Hybrid matrices reinforced with glass beads were also tested through SEM. Next Figures 27 and 28 show SEM images derived from 80% marble sand–20% epoxy resin

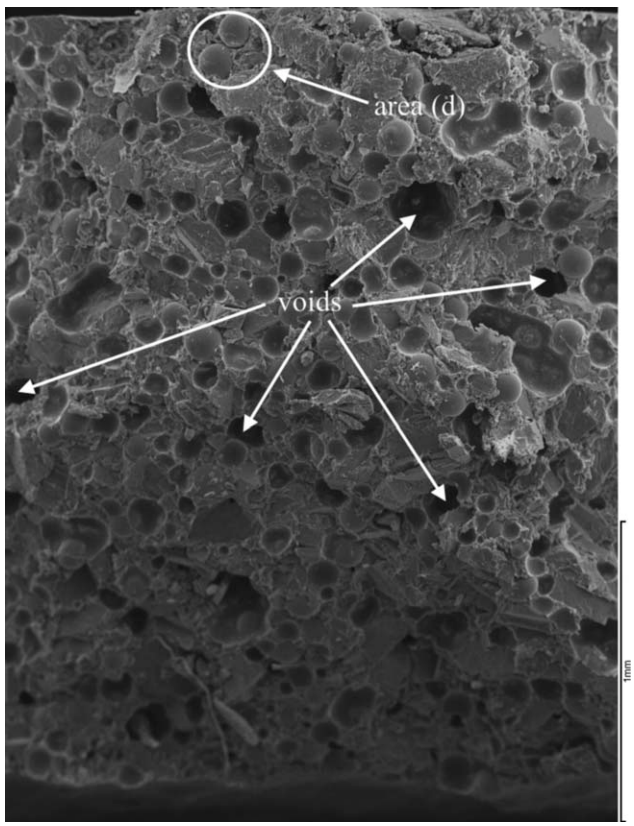

Figure 28 SEM image: Fracture surface cross section of hybrid matrix consisting of 80% marble sand and 20% epoxy resin reinforced with 30 wt % glass beads.

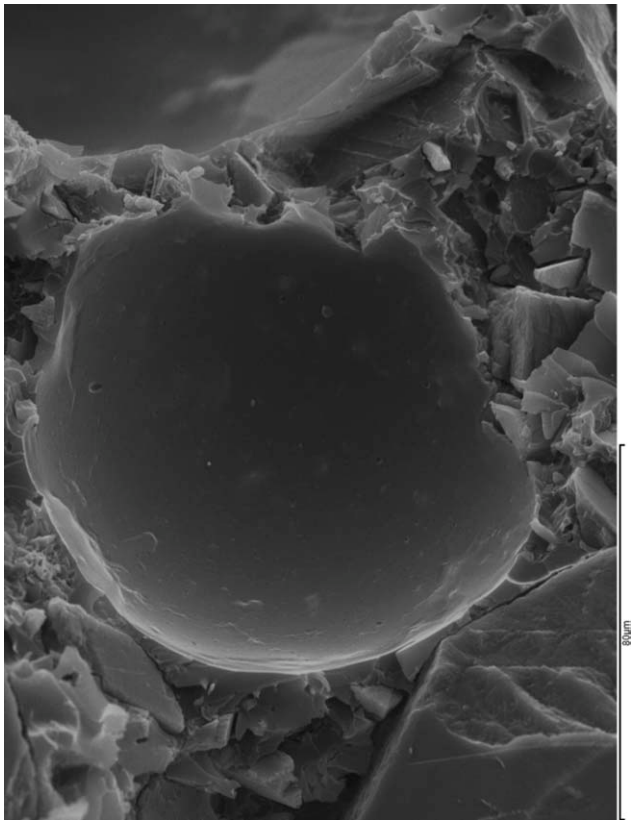

Figure 29 SEM image: Area (c)

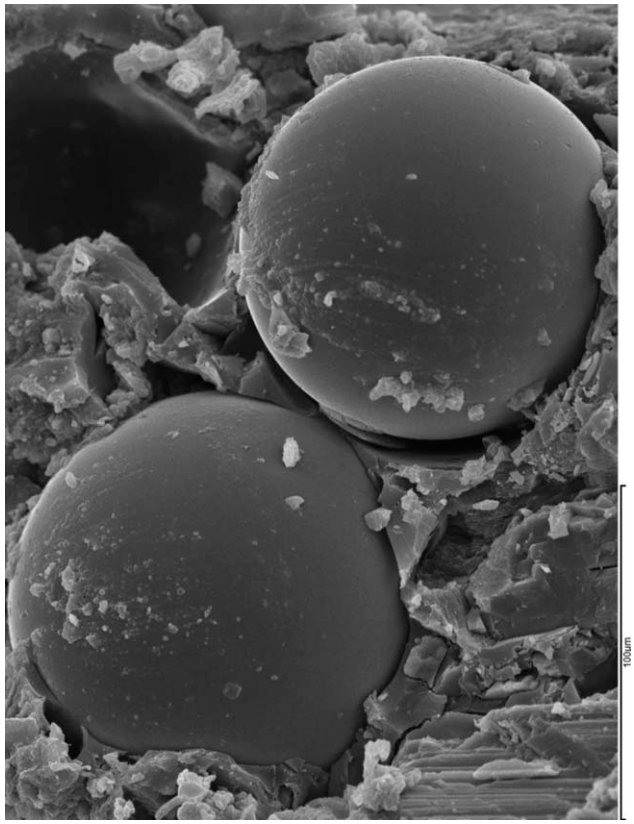

Figure 30 SEM image: Area (d)

hybrid matrices reinforced with 5 and 30% by weight glass beads content, respectively. Good distribution of the reinforcement is obvious in both cases, while there is no sign of extensive agglomerations even at the composition with the highest reinforcement loading. Nevertheless, higher reinforcement loading makes void's presence more frequent in the mass of the composite as it can be seen on Figure 28.

Magnification over the areas designated as "area c" and "area d" on Figures 27 and 28 show good adhesion between resin and glass beads. Figure 29 shows the magnification of "area c" (80% marble sand–20% epoxy resin hybrid matrix reinforced with 5 wt % glass beads), where a glass bead was debonded leaving its trace on smooth resin substrate which the nonporous texture of it denotes good adhesion conditions between matrix and reinforcement.

Good adhesion conditions between matrix and glass beads can be observed in Figure 30, which shows a magnified SEM image of area "d" (80% marble sand–20% epoxy resin hybrid matrix reinforced with 30 wt % glass beads). The difference is that in that case higher reinforcement load caused a more intense presence of voids in the matrix something that gives an explanation for the degradation on the strength of the composite, which was experimentally observed.

Hybrid matrices with steel fibers reinforcement

Figures 31 and 32 depict the fracture surface cross section of hybrid matrices consisting of 60% marble sand–40% epoxy resin and 70% marble sand–30% epoxy resin, respectively, reinforced with 5 wt % steel fibers. As it can be observed in both figures, high specific weight of steel leads to sparse presence of fibers in a specimen's cross section. This

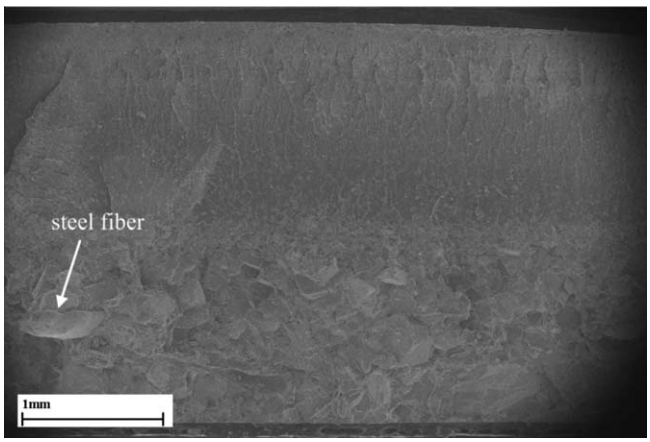

Figure 31 SEM image: Fracture surface cross section of hybrid matrix consisting of 60% marble sand and 40% epoxy resin reinforced with 5 wt % steel fibers.

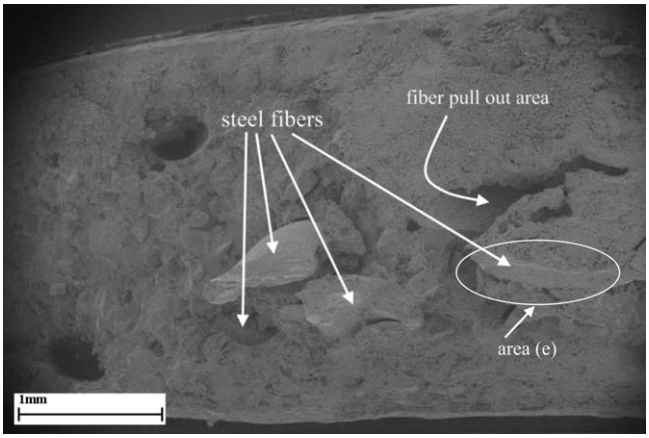

Figure 32 SEM image: Fracture surface cross section of hybrid matrix consisting of 70% marble sand and 30% epoxy resin reinforced with 5 wt % steel fibers.

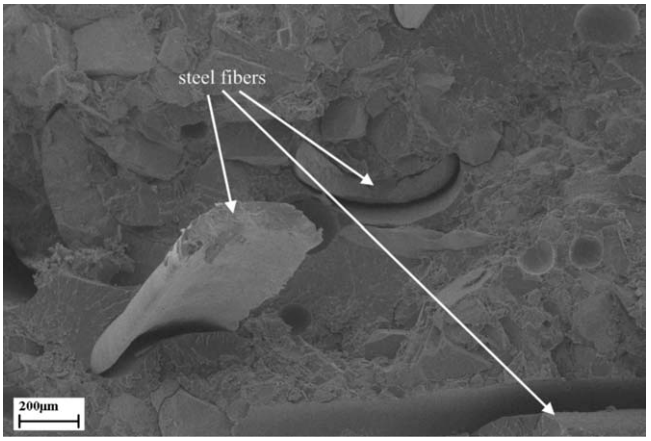

Figure 34 SEM image: Fracture surface cross section of hybrid matrix consisting of 70% marble sand and 30% epoxy resin reinforced with 20 wt % steel fibers.

observation comes to agreement with experimental results that showed that steel fibers presence does not have any effect on the composite's mechanical behavior until a critical, by weight, loading is added.

As discussed before, optimum mechanical properties for both hybrid matrices were derived from 20% by weight steel fibers loading. Figures 33 and 34 show fracture surface cross sections for both hybrid matrices examined, reinforced with 20% by weight steel fibers. As it can be seen higher reinforcement content does not affect the hybrid matrix quality since no voids or discontinuities can be observed through image observation. Moreover, as Figure 35 shows, fibers and matrix seem to have good adhesion conditions for the 60% marble sand–40% epoxy resin hybrid matrix.

The same can be obtained from Figure 36, where a more detailed SEM image shows a crack on 70% marble sand–30% epoxy resin hybrid matrix in the vicinity of a steel fiber. In this case, though fiber had debonded, this seems to be due to the propagation through the fiber-matrix interface of the crack that was created in the matrix.

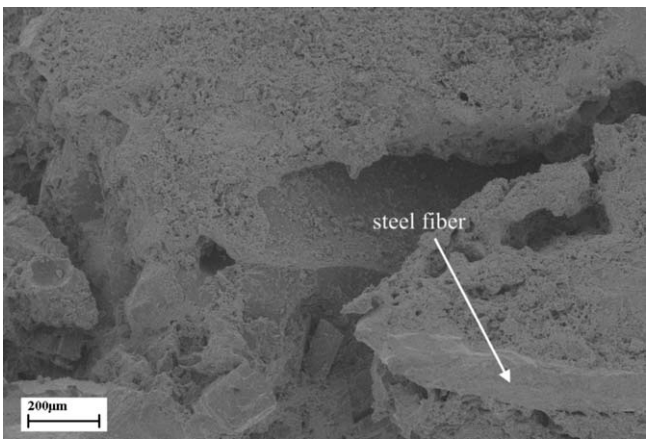

Figure 35 SEM image: Area (e)

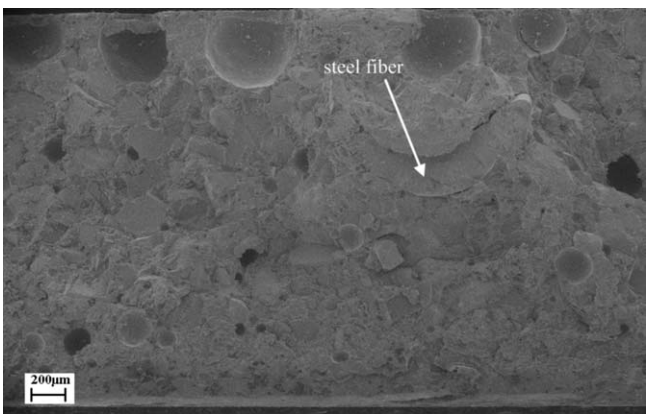

Figure 33 SEM image: Fracture surface cross section of hybrid matrix consisting of 60% marble sand and 40% epoxy resin reinforced with 20 wt % steel fibers.

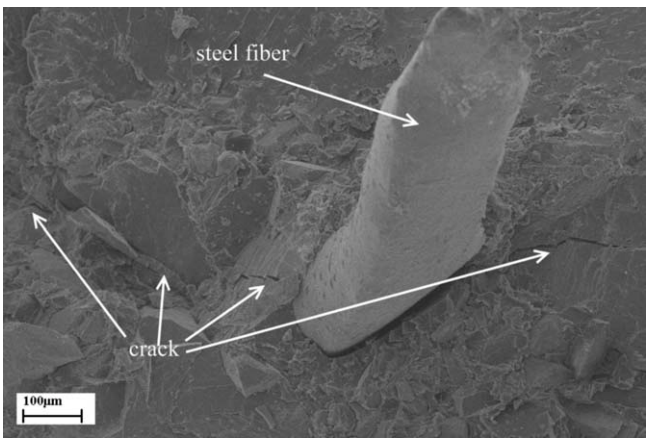

Figure 36 SEM image: Detailed image on fracture surface cross section of hybrid matrix consisting of 70% marble sand and 30% epoxy resin reinforced with 20 wt % steel fibers.

CONCLUSIONS

In this investigation various compositions of epoxy resin/fine marble sand hybrid matrix composites reinforced with short glass fibers, glass beads and short steel fibers were mechanically tested in three-point bending tests according to ASTM D790-99 standards to investigate their mechanical flexural properties and behavior.

Glass fibers were found to be not an appropriate reinforcement for this kind of matrix and perhaps the method of mixing applied.

Glass beads on the other hand, had a strong reinforcing effect on the stiffness of the composite when high beads content, up to 30% by weight, was added; nevertheless for such high beads content, flexural strength was degrading to values lower than the respective one of unreinforced matrix.

Finally, steel fibers addition to the matrix, led to composites with enhanced stiffness and flexural strength. Stiffness was found to increase 68% comparing to the stiffness of the unreinforced matrices while flexural strength was found to increase up to 28% comparing to the flexural strength measured from the corresponding unreinforced matrix. The enhancement of both properties occurred for the same fiber content, by weight, which was found to be that of 20 wt %, and this is the main reason for which steel fibers can be considered as the most effective type of reinforcement from those tested.

References

1. Micelli, F.; Nanni, A. Constr Build Mater 2004, 18, 491.
2. Kulakowski, M. P.; Pereira, F. M.; Molin, D. C. C. D. Constr Build Mater 2009, 23, 1189.
3. Issa, C. A.; Debs, P. Constr Build Mater 2007, 21, 157.
4. Colomb, F.; Tobbi, H.; Ferrier, E.; Hamelin, P. Compos Struct 2008, 82, 475.
5. Li, Y-F.; Xie, Y-M.; Tsai, M-J. Constr Build Mater 2009, 23, 411.
6. Seica, M. V.; Packer, J. A. Compos Struct 2007, 80, 440.
7. Corradi, M.; Grazini, A.; Borri, A. Compos Sci Technol 2007, 67, 1772.
8. Reis, J. M. L.; Ferreira, A. J. M. Build Environ 2006, 41, 262.
9. Täljsten, B. Constr Build Mater 2003, 17, 15.
10. Zhang, B.; Masmoudi, R.; Benmokrane, B. Constr Build Mater 2004, 18, 625.
11. Czaderski, C.; Motavalli, M. Compos Part B-Eng 2004, 35, 279.
12. Moon, D. Y.; Sim, J.; Oh, H.; Benmokrane, B. Compos Part B-Eng 2008, 39, 882.
13. Hull, D. An Introduction to Composite Materials; Cambridge University Press: Cambridge, 1981.